ARTICLE

Investigating the Outskirts of Fe and Co Catalyst Particles in Alumina-Supported Catalytic CVD Carbon Nanotube Growth

Mark H. Rümmeli,[†,‡,*] Franziska Schäffel,[†] Alicja Bachmatiuk,[†] David Adebimpe,[§] Geoff Trotter,[∥] Felix Börrnert,[†] Andrew Scott,[†,⊥] Emica Coric,[†] Maria Sparing,[†] Bernd Rellinghaus,[†] Paul G. McCormick,[∥] Gianaurelio Cuniberti,[⊥] Martin Knupfer,[†] Ludwig Schultz,[†] and Bernd Büchner[†]

[†]IFW Dresden, P.O. Box 270116, D-01171 Dresden, Germany, [‡]Department of Physics, Dresden University of Technology, D-01062 Dresden, Germany, [§]Polymath Interscience, LLC, 3 Church Circle, Suite 366, Annapolis, Maryland 21401, [∥]Antaria Limited, 10/3 Brodie Hall Drive, Technology Park Bentley, WA 6102 Australia, and [⊥]Institute for Materials Science and Max Bergmann Centre of Biomaterials, Dresden University of Technology, D-01062 Dresden, Germany

ABSTRACT Using thermal CVD, the synthesis of multi-walled carbon nanotubes exhibiting roots anchored directly onto α-alumina supports, rather than the catalyst particle, is reported. At such roots, the alignment of the graphitic planes with the support lattice fringes depends on the support crystal structure and orientation. Surface defects may alter the reactivity of the surface or control the anchoring of supported atoms or nanoparticles. We argue this surface defect is provided by the catalyst particle's edge interaction with the support, in other words its circumference. The development of oxide-based catalysts is attractive in that they potentially provide an appropriate solution to directly integrate the synthesis of carbon nanotubes and graphene into silicon-based technology.

KEYWORDS: carbon nanotube · growth · catalysts · oxides · synthesis · CVD

*Address correspondence to m.ruemmeli@ifw-dresden.de.

Received for review November 12, 2009 and accepted January 12, 2010.

Published online January 20, 2010. 10.1021/nn9016108

It is without doubt that the developments and advancements over the last two decades in the discovery and application of carbon structures at the nanoscale have captivated the imagination of scientists and engineers. This was triggered by the discovery of buckminster fullerenes by H. Kroto, R.E. Smalley, and R.F. Curl,[1] in which carbon hexagon and pentagon structures formed a round structure much like a football. This prompted various advances in their synthesis, which ultimately led to Iijima presenting beautiful transmission electron microscopy (TEM) images of multi-walled carbon nanotubes (MWNTs)[2] and their revelation as concentric tubes of rolled up graphite with enormous mechanical strength. This was followed with the discovery of carbon nanotubes with one wall, aptly called single-walled carbon nanotubes (SWNTs).[3,4] SWNTs have rather special properties in that, depending on how the graphene (single layer of graphite) forming them is rolled up, it can be either metallic or semiconducting.[5] They show considerable promise as components in molecular electronics,[6] and huge resources are being ploughed into their development. Recently though, graphene (single layer graphite) has emerged as the new star.[7] The two-dimensional material is stable under ambient conditions and is in many ways a competitor to SWNTs. This is because SWNTs are essentially graphene ribbons rolled into a cylindrical shape, and their properties are due to the confinement of electrons. The width of a graphene ribbon confines the electrons in a similar manner controlling the materials' band gap. Thus, the promise of carbon-based nanoelectronics now includes graphene.

A stumbling block for carbon nanotubes has been their controlled synthesis in terms of their diameter and chirality since this determines their band gap. This same handling restriction will also apply to graphene, at least to some degree. Hence, if carbon nanostructures are to truly realize their potential in molecular electronics, a clear understanding of the mechanisms involved in their synthesis at an atomic scale is required.

By far, most successful routes for carbon nanotube synthesis use metal catalyst particles for their formation and some even argue, albeit falsely, that carbon nanotubes can only be synthesized with metal catalysts, despite Iijima's[2] initial work synthesizing MWNTs without the aid of catalyst particles. This belief arose due to the discovery of SWNTs occurring through the use of metal catalysts.[3,4] MWNTs can also be formed with metal catalysts. Further, the use of metal catalysts could be applied over a variety of synthesis routes including arc-discharge, laser evaporation, high pressure

carbon monoxide process (HiPCO), and chemical vapor deposition (CVD). The simplicity and economic efficiency of metal-catalyzed CVD nanotube growth, which can be accomplished both in floating catalyst[8] and in supported catalyst configurations,[9] have led to catalytic CVD establishing itself as the synthesis route of choice. Hence studies on the growth of carbon nanotubes focus almost exclusively on the catalyst particle where it is argued its role is to provide the initial embryonic cap of a tube (nucleation), continually supply carbon to the root end (growth), and in CVD, it is also supposed to catalytically decompose the carbon feedstock (usually a hydrocarbon).

Despite disparate studies and many advances, there remain many unclear issues and contradictions, not least the (contentious) requirement of a metal catalyst particle. Initially, it was argued that only transition metals could be used (*e.g.*, Fe, Ni, Co, Pt); however, various studies over the past few years show that a whole host of atypical metals such as Cu, In, Pb, Au, Ag, Mg, Al, Cr, Mo, Sn, and Mn can be used in CNT formation.[10−12] Many of these metals require activation through oxygen.[10,11] In addition, the use of ceramics as catalysts began to emerge and include Si, Ge, and SiC.[13] It is worth noting that the use of SiC for CNT synthesis *via* the high temperature decomposition of SiC requires oxygen in the reaction.[14] In addition, the use of metal oxide catalysts[10,15−17] is emerging as an attractive alternative to metal catalysts due to their potential integration with Si technology and easier removal from as-produced CNT samples (purification). The catalytic activity of metal oxides opens up a key question as to whether the oxides, when used as supports for metal catalysts in CNT synthesis, play an active catalytic role in the formation of the CNT.

In this study, we investigate CVD-grown CNTs from Fe and Co catalysts supported on alumina. Various studies, including detailed electron microscopy studies, show the graphitic walls of the CNTs do not terminate on the catalyst particle but lie outside the catalyst particle. They are observed to terminate on the alumina support and align themselves with the lattice fringes of the oxide support. Our findings point to nucleation occurring through the metal catalyst particle while growth apparently occurs from the alumina support itself.

RESULTS AND DISCUSSION

Numerous works highlight a strong correlation between the diameters of the catalyst and that of the resultant carbon nanotube.[8,16,18] In addition, at least for iron catalyst nanoparticles, it has been shown that the number of walls a tube forms increases with increasing catalyst particle size.[16] This study shows a similar correlation between catalyst diameter and number of engendered tube walls for Co, as found with Fe, and both

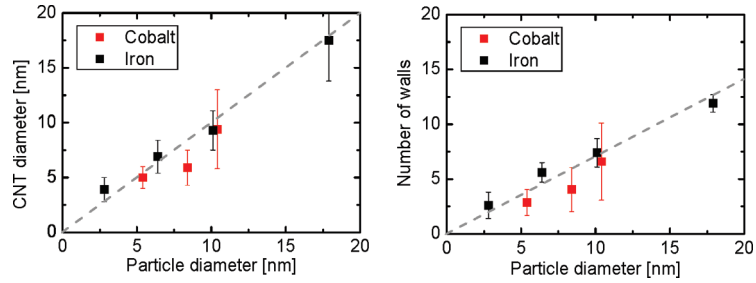

Figure 1. Left panel: mean CNT outer diameter against catalyst particle size for Fe (black) and Co (red). Right panel: mean number of walls *versus* catalyst particle size Fe (black) and Co (red). Dashed lines are a guide to the eye. All samples were synthesized at 750 °C with cyclohexane as the carbon source (5 min) after pretreatment in H_2 (5 min).

are illustrated in Figure 1. Our data are qualitatively well-supported by the volume-to-surface area model,[16,19] in which the outer tube diameter and number of walls are dictated by the amount of carbon available from a carbon-saturated catalyst particle at the point of nucleation. During nucleation, the available carbon precipitates to form a hemispherical nucleation cap (yarmulke).[20] Once an initial cap has formed, consecutive caps form within the initial cap (squeezing the catalyst particle) until the dissolved carbon is exhausted. This process is dependent on the catalyst volume-to-surface area ratio since the carbon availability at nucleation is determined by the catalyst volume while the carbon usage for cap formation is area-dependent.

A critical issue is that once the initial caps have formed (nucleation) where does the root of a growing nanotube lie? *In situ* TEM studies show the root of a growing nanotube can interface with the catalyst particle.[21,22] Other studies, although claiming growth from the catalyst particle, provide some TEM images that are not so clear, that they may even be interpreted as evidencing the root of graphitic walls being attached to the support.[23,24] Recent TEM observations at 300 kV also suggest the root of a carbon nanotube can lie at the oxide support as opposed to the catalyst.[16] To better determine the interface between the tube, catalyst, and support, we implemented a series of studies using low-voltage third-order aberration-corrected TEM to study the roots of carbon nanotubes on a variety of supports, namely, Al_2O_3, TiN, and graphite. The results are striking and show that nanotube growth does not always occur at the catalyst.

Figure 2 (left and middle panels) shows the root of a multi-walled carbon nanotube grown on 10 nm Al_2O_3 on Si/SiO_2. The Al_2O_3 film has been removed, and the TEM image was acquired with the film perpendicular to the electron beam. The concentric rings at the root of the tube are seen to lie directly on the Al_2O_3 film, and the catalyst particle clearly sits entirely in the core of the tube. This is concomitant with previous studies indicating the root ends of a MWNT lie outside the catalyst particle, *viz.* the graphitic planes do not root on

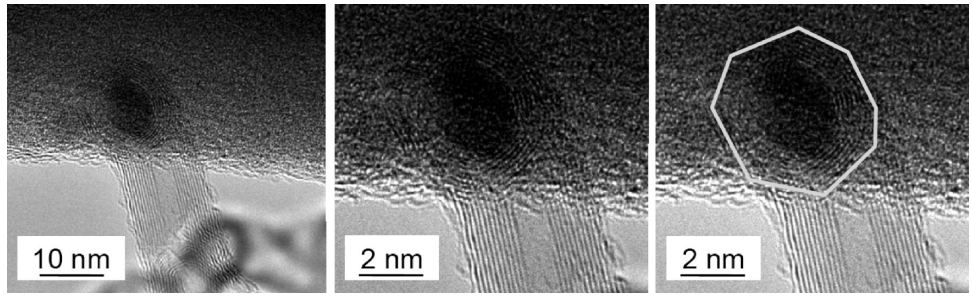

Figure 2. TEM micrographs showing the root of a CNT residing on the surface of Al_2O_3 (after removal from the Si/SiO_2 wafer). The middle and right panels show the root at higher magnification. The graphitic walls reside on the Al_2O_3 support, while the catalyst particle sits entirely within the core of the CNT. The right panel highlights the polygon structure of the outer (larger diameter) CNT walls residing on the alumina surface. The inner walls are more circular.

the particle. The catalyst particle itself is elongated and resides in the core of the tube.[16] Further studies with cleaved $Si/SiO_2/Al_2O_3$/CNT samples with the tube growth oriented perpendicular to the electron beam were also conducted. Of the observed carbon nanotube roots, the images appeared to show the graphitic walls merging into the support; however, we were unsuccessful in obtaining clear images of the interface between the tube end and support. To overcome this technical limitation, we grew the nanotubes directly on α-Al_2O_3 nanoplatelets (*i.e.*, the thin edge of the platelet is 100 nm or less for transmission). The catalyst particles, as with all experiments in this study, were deposited *via* a gas phase deposition route.[18] Figure 3 (upper left and right and bottom left) shows typical carbon nanotube growth on the nanoplatelets after being subjected to a CVD reaction with cyclohexane as the feedstock. The CVD reaction results in the formation of graphite-encapsulated (fully and partially) catalyst particles, carbon nanotubes, and few-layer graphene formation (Figure 3 bottom right) on the surface of the Al_2O_3 nanoplatelets. Catalyst particles on the thin edge of the platelets which grow carbon nanotubes are good

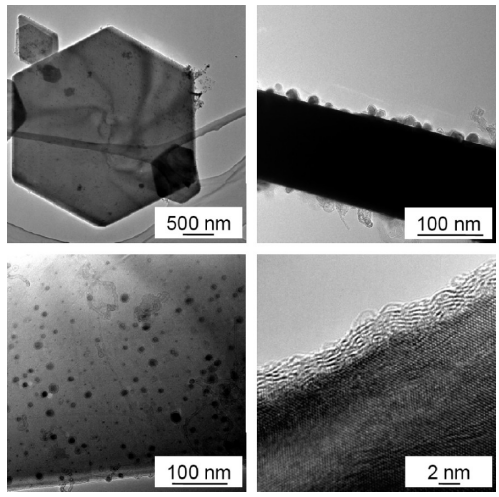

Figure 3. TEM micrographs showing α-alumina nanoplatelets. Basal and side view (top left and right images, respectively). The bottom left and right images show CNT and catalyst particles on the nanoplatelet surface and few-layer graphene on the surface, respectively.

candidates for providing cross-sectional TEM views of the root of a carbon nanotube. An example of such a view is presented in Figure 4. The micrograph shows an elongated catalyst particle (Co in this case) residing on the edge of an α-Al_2O_3 platelet (support). The lattice fringes from the α-Al_2O_3 support are clearly visible. Graphitic structures can also be seen to emanate from the tip of the catalyst particle. However, more importantly though, the outer walls of the carbon nanotube are seen to align themselves with the lattice fringes of the Al_2O_3, and it is clearly evident that the graphitic walls connect directly with the Al_2O_3 crystal and not the catalyst. The middle and right images presented in Figure 4 highlight the alignment of the graphitic walls with the lattice fringes. The graphite lattice orientation is parallel to the rhombohedral Al_2O_3 (100) lattice fringes. At the interface boundary, the graphite wall spacing deviates a little from the graphite lattice spacing (d_{0002g} = 0.34 nm) so as to align with each second Al_2O_3 lattice plane (d_{110} = 0.238 nm). In some instances, the graphitic planes bend to align themselves with the Al_2O_3 lattice plane. This bending behavior has been observed with CNT/FeCo interfaces.[21] The alignment of the graphitic planes depends on the relative orientation between the tube walls and the support crystal orientation. In Figure S1 (see Supporting Information), the alumina lattice fringes again correspond to the (110) lattice plane. The angle between the graphite walls on the left side of the catalyst particle and the Al_2O_3 (110) lattice fringes is 150°. For the most part, the graphitic walls anchor at consecutive fringes. The alumina lattice fringes are at 30° to the alumina surface plane, and this leads to a spacing at the surface between fringes being twice the actual (110) lattice spacing ($2 \times 0.238 = 0.476$ nm). Hence, this is almost the same spacing as found with the case illustrated in Figure 4, in which the graphitic walls aligned with every second (110) lattice fringe. No expansion between alumina lattice fringes toward the surface is observed. Further, at the interface, the graphitic planes bend to align themselves with the alumina lattice fringes to varying degrees. This occurs in order to compensate for the difference in spacing between the CNT walls and the lattice spacing at the support sur-

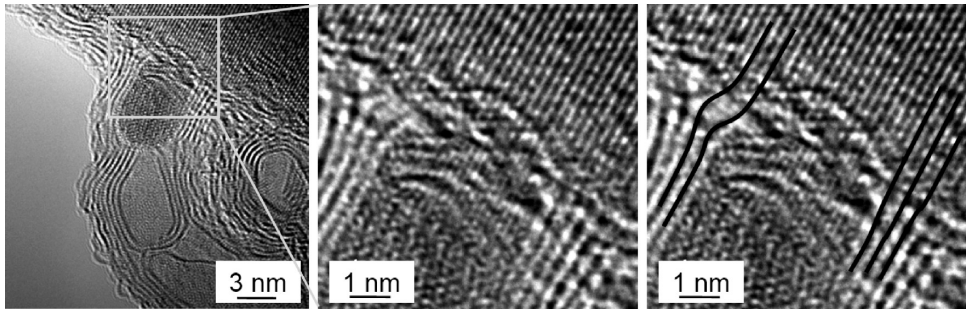

Figure 4. TEM micrographs showing cross-section view of a CNT root at the support surface. The (Co) catalyst particle resides in the core of the tube. The fringes at the base of the particle correspond to the (200) lattice fringes of cubic Co. The outer walls of the CNT align themselves with the lattice fringes of the α-alumina nanoplatelet. The middle micrograph is a magnification of the boxed region from the left micrograph. The right micrograph is a copy of the middle image with lines added to highlight the alignment of the graphitic planes with the rhombohedral (110) lattice fringes of the corundum support.

face while seeking to minimize strain energy. To underscore the anchoring of the graphitic walls, it is worth viewing the movie provided in the Supporting Information. In it, a series of TEM images from the root shown in Figure S1 are collated as a movie. The graphitic walls of the CNT are seen to wiggle due to the electron irradiation; however, the roots of the graphitic walls at the support interface remain steadfastly locked on to the support.

It should be borne in mind that the presented micrographs are 2D cross sections. In reality, the circular form of each concentric root forming the CNT will adjust its anchor point so as to minimize its strain energy and will be dependent on the support crystal structure and orientation, phase, and material. The process of minimizing strain energy can explain the polygon structure of the outer walls (larger diameter) seen in top views of the tube roots, as, for example, shown in the right panel of Figure 2. In addition, the periodicity of the tube wall alignment with the lattice fringes is sometimes observed to be broken; that is, in cases with consecutive alignment, a fringe might be skipped, or where fringes were periodically skipped, a consecutive fringe would be adopted as an anchor point. Again, this can be fully explained in terms of minimizing strain energy due to geometrical considerations.

The use of different non-oxide supports, namely, TiN and graphite, leads to very different nanotube formation. In both cases, few, if any, tubes with parallel walls are obtained. Instead, the structures contain many pockets stacked upon each other and often contain catalyst material residing within various places along their length. The structures appear disordered, and their mean diameters and diameter distributions are significantly larger than those from the starting catalyst particles (*e.g.*, catalyst particles range = 4−12 nm, CNT diameters on TiN range = 10−140 nm, and CNT diameters on graphite = 10−80 nm). This indicates the occurrence of coalescence. The obtained structures are distinct from those found on the alumina support in which the diameters and diameter distributions of as-produced CNT match those of the starting catalyst diameters (Figure 1). In addition, the produced tubes form with parallel walls almost entirely along their length, particularly when using Fe as the catalyst in comparison to Co. The different morphologies obtained from the different supports are shown in Figure S2 in the Supporting Information.

The use of graphite as a support is particularly interesting despite leading to the formation of disordered carbon nanostructures, in agreement with studies by Yacamán *et al.*[25] The ease with which one can cleave relatively few graphitic layers affords facile sample preparations for TEM studies. This is seen in Figure 5, in which a bamboo-like carbon nanotube is imaged at various magnifications. The bamboo structure is clearly

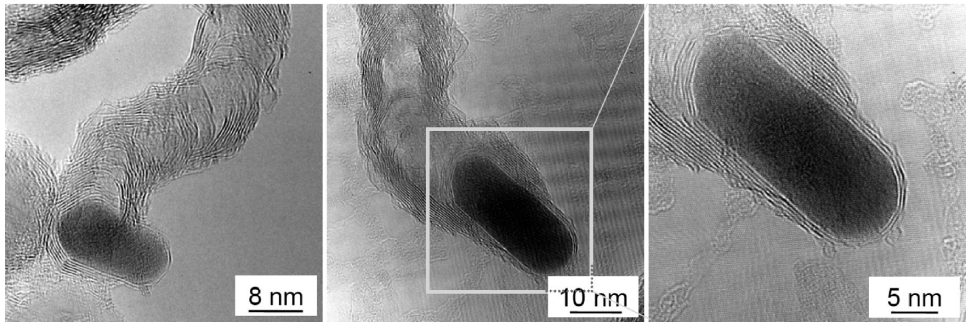

Figure 5. TEM micrographs showing a typical bamboo-like CNT grown on graphite (left and middle panels). The right panel is a magnification of the boxed region in the middle panel and highlights the cap-like graphitic structures terminating outside the elongated catalyst particle.

observed to have been formed by the stacking of cup (or cap) structures. The root of the bamboo-like tube shows an elongated catalyst particle, and most importantly, the ends of the cap-like structures forming the tube lie outside the catalyst particle. They do not terminate on the catalyst particle and highlight how catalyst cap formation can occur externally to the catalyst particle, which can then root to an appropriate support, such as alumina.

The presented findings clearly evidence graphitic nanotube walls rooted on oxide (alumina) supports as opposed to the catalyst particle. The nanotubes grown on alumina, in general, comprise parallel walls with few structural disorders (*e.g.*, pocket formation as obtained in bamboo-like CNT). The tube diameters and diameter distributions show a direct correlation with that of the pristine catalyst particles for both Fe and Co catalysts. CNTs grown in identical CVD conditions on TiN and graphite have diameters that show no correlation with the pristine catalyst particles, and no walls are observed to root into the supports. The carbon nanostructures are highly disordered and do not have parallel walls with a hollow core. The ends of the bamboo-like or stacked cup-like structures formed from catalysts residing on graphite allowed detailed TEM studies which show multicap formation with the roots lying outside the catalyst particle; furthermore, the catalyst particle itself is elongated.

Preliminary studies of ours using Fe catalysts indirectly pointed toward oxide-driven growth of carbon nanotubes. In those studies, the tops of the nanotubes were capped, and the roots were open-ended and appeared to reside directly on the substrate while the catalyst particles were elongated and were observed at various locations along the length of the nanotube. All of these observations we also find when using Co catalysts supported on alumina (see Figure S3).

The findings fit with the previously proposed volume-to-surface area model,[19] which states that for supported catalysts the number of caps (and hence walls) formed at nucleation depends on the available carbon precipitating from the catalyst particle at nucleation. Since encapsulation is unlikely due to the interaction with the support, multiple caps will form. At this stage, two possible scenarios can occur: the roots of the caps lie at the catalyst particle[21,22] or the roots lie externally to the catalyst particle, such that each time a new cap is formed within the previous the catalyst particle is compressed and elongated. In this later scenario, passivation of unsaturated bonds at the end of the caps is energetically favored. This can be achieved by anchoring into an oxide support. Oxides are key components for a variety of catalytic reactions, functioning directly as reactive components or as supports for dispersed metal species or as additives or promoters to enhance the rate of catalytic reactions.[26] Yet remarkably, in carbon nanotube synthesis, their potential role is seldom posited beyond the strong interaction between the catalyst particle and support which minimizes coalescence.

Since the presented data show that graphitic walls from a carbon nanotube can interact directly with the oxide support, it is worth considering what processes may be active. The catalytic activity of oxide surfaces is not fully understood; however, certain aspects are relatively well-comprehended. For example, it is known that defects are usually responsible for many of the catalytic and chemical properties. This usually occurs through point defects, steps, and kinks on oxide surfaces, and they have been shown to dissociate H−H, C−H, C−C, C═O, and O═O bonds.[26,27] Surface defects can alter the reactivity of the surface or control the anchoring of supported atoms or nanoparticles. Defect sites on oxides in CVD reactions of the type used for carbon nanotube synthesis have previously been implicated in the observed graphitic anchoring and formation with the graphitic layers formed on the crystalline oxide particles shown to root at step sites.[28] While it is easy to envisage a step site serving as the active region for graphene formation, it is less clear how a defect site for a nanotube might occur. This is where the catalyst particle provides a role beyond cap formation. The periphery of the catalyst particle and the support in essence form a circular (or polygon) defect on the surface of the substrate. Indeed, the periphery in many supported catalysts on oxides provides a key catalytic active region. One of the most notable examples is the heterogeneous catalytic activity of gold. It is usually argued that the Au atoms at the interface between the Au particle and the oxide are the active oxidation centers (see ref 26 and references within). It is worth remembering that the synthesis of carbon nanotubes *via* the decomposition of SiC requires trace amounts of oxygen. Oxygen has been shown to exist at the surface of the SiC where the sp^2 carbon anchors onto the crystal.[14,29] The evidence presented here shows a direct interaction between the graphitic roots of a carbon nanotube and an α-alumina support. On the basis of these findings, it cannot be exclusively decided if carbon preferentially binds at oxygen sites. However, the argument for oxygen is compelling because oxygen is known to enhance graphitization and activate catalysts in CNT formation.[10,14,30] Furthermore, as we have shown, the use of non-oxide supports results in the formation of non-uniform structures. The need to replenish oxygen at the substrate surface would offer an additional explanation for the role of H_2O in the supergrowth of CNTs.[31,32] For example, water reacts very efficiently with Al-terminated surfaces on Al_2O_3, where it dissociates, resulting in surface hydroxyl groups (see ref 33 and references therein). It is also well-known that oxygen centers are active in catalyzing many organic chemistry reactions, such as the Michael-type addition.

CONCLUSION

To summarize, we have demonstrated the rational synthesis of CNTs exhibiting roots anchored onto α-alumina. At the roots, the alignment of the graphitic planes depends on the support crystal structure, orientation, phase, and strain energy minimization. Further studies are required to clarify the nature in which the graphitic planes anchor at the atomic level. The central finding that graphitic structures interface with oxides has serious implications because it paves the way for both carbon nanotubes and graphene to be directly integrated into silicon technology.

EXPERIMENTAL SECTION

The catalyst nanoparticles were prepared using an inert gas condensation magnetron sputtering system. Fe or Co targets in an Ar and/or He atmosphere were used.[18] The catalyst particles were deposited onto thermally oxidized silicon substrates with 10 nm Al_2O_3 surface layers or 100 nm TiN layers (Samsung), high purity graphite (Goodfellows) or α-alumina nanoplatelets. To obtain *a priori* information on the deposited catalyst particles, they were simultaneously deposited onto carbon-coated transmission electron microscopy (TEM) grids which served as witness plates. The integrity of the witness plates was confirmed by atomic force microscopy (AFM) studies of deposited particles on several $Si/SiO_2/Al_2O_3$ substrates. The CVD syntheses were conducted on a purpose-built horizontal tube furnace, in which the furnace can be slid onto or off the reaction zone. The protocol for the CVD reaction is as follows: Initially, the system is evacuated to 1 mbar through a membrane pump. The particles are then reduced in dynamic hydrogen (40 sccm, 40 mbar) for 5 min at a temperature of 800 °C. Thereafter, the system was again evacuated, and then cyclohexane was introduced to a pressure of 50 mbar. The reaction was run for 5 min, after which the oven was slid away from the reaction zone and the reaction chamber was evacuated. The system was then cooled by flowing water over the reaction zone until the temperature fell below 150 °C, after which the samples were then removed for various analyses. Structural and morphological information was obtained with TEM on a third-order spherical aberration-corrected FEI Titan 80-300 providing sub-angstrom resolution and operating at 80 kV to minimize knock-on damage. AFM studies were conducted on a Digital Instruments 3100 (lateral resolution <5 nm, vertical resolution <1 nm).

Acknowledgment. F.S. acknowledges funding from the Cusanuswerk. A.B. thanks the EU for a MC fellowship (CARBIO). A.S. thanks the EU for support *via* its ERASMUS program. M.H.R. thanks the EU and the Free State of Saxony for support *via* ECEMP. We are grateful to Dr. Subramanya Mayya (Samsung) for supplying TiN substartes, and R. Schönfelder, S. Leger, and R. Hübel for technical support.

Supporting Information Available: Additional figures and movie. This material is available free of charge *via* the Internet at http://pubs.acs.org.

REFERENCES AND NOTES

1. Kroto, H. W.; Heath, J. R.; O'Brien, S. C.; Curl, R. F.; Smalley, R. E. C60: Buckminsterfullerene. *Nature* **1985**, *318*, 162–163.
2. Iijima, S. Helical Microtubules of Graphitic Carbon. *Nature* **1991**, *354*, 56–58.
3. Bethune, D.; Kiang, C.-H.; de Vries, M.; Gorman, G.; Savoy, R.; Vazquez, J.; Beyers, R. Cobalt-Catalysed Growth of Carbon Nanotubes with Single-Atomic-Layer Walls. *Nature* **1993**, *363*, 605–607.
4. Iijima, S. Single-Shell Carbon Nanotubes of 1-nm Diameter. *Nature* **1993**, *363*, 603–605.
5. Hamada, N.; Sawada, S.; Oshiyama, A. New One-Dimensional Conductors: Graphitic Microtubules. *Phys. Rev. Lett.* **1992**, *68*, 1579–1581.
6. Baughman, R. H.; Zakhidov, A. A.; de Heer, W. A. Carbon Nanotubes—The Route toward Applications. *Science* **2002**, *297*, 787–792.
7. Novoselov, K. S.; Geim, A. K.; Morozov, S. V.; Jiang, D.; Zhang, Y.; Dubonos, S. V.; Grigorieva, I. V.; Firsov, A. A. Electric Field Effect in Atomically Thin Carbon Films. *Science* **2004**, *306*, 666–669.
8. Cassell, A. M.; Raymakers, J. A.; Kong, J.; Dai, H. Large Scale CVD Synthesis of Single-Walled Carbon Nanotubes. *J. Phys. Chem. B* **1999**, *103*, 6484–6492.
9. Li, W. Z.; Xie, S. S.; Qian, L. X.; Chang, B. H.; Zou, B. S.; Zhou, W. Y.; Zhao, R. A.; Wang, G. Large-Scale Synthesis of Aligned Carbon Nanotubes. *Science* **1996**, *274*, 1701–1703.
10. Rümmeli, M. H.; Borowiak-Palen, E.; Gemming, T.; Pichler, T.; Knupfer, M.; Kalbac, M.; Dunsch, L.; Jost, O.; Silva, S.; Pompe, W.; *et al.* Novel Catalysts, Room Temperature and the Importance of Oxygen for the Synthesis of Single Wall Carbon Nanotubes. *Nano Lett.* **2005**, *5*, 1209–1215.
11. Takagi, D.; Homma, Y.; Hibino, H.; Suzuki, S.; Kobayashi, Y. Single-Walled Carbon Nanotube Growth from Highly Activated Metal Nanoparticles. *Nano Lett.* **2006**, *6*, 2642–2645.
12. Yuan, D.; Ding, L.; Chu, H.; Feng, Y.; McNicholas, T.; Liu, J. Horizontally Aligned Single-Walled Carbon Nanotube on Quartz from a Large Variety of Metal Catalysts. *Nano Lett.* **2008**, *8*, 2576–2579.
13. Takagi, D.; Hibino, H.; Suzuki, S.; Kobayashi, Y.; Homma, Y. Carbon Nanotube Growth from Semiconductor Nanoparticles. *Nano Lett.* **2007**, *7*, 2272–2275.
14. Kusunoki, M.; Suzuki, T.; Kaneko, K.; Ito, M. Formation of Self-Aligned Carbon Nanotube Films by Surface Decomposition of Silicon Carbide. *Philos. Mag. Lett.* **1999**, *79*, 153–161.
15. Liu, B.; Ren, W.; Gao, L.; Li, S.; Pei, S.; Liu, C.; Jiang, C.; Cheng, H. M. Metal-Catalyst-Free Growth of Single-Walled Carbon Nanotubes. *J. Am. Chem. Soc.* **2009**, *131*, 2082–2083.
16. Rümmeli, M. H.; Schäffel, F.; Kramberger, C.; Gemming, T.; Bachmatiuk, A.; Kalenczuk, R.; Rellinghaus, B.; Büchner, B.; Pichler, T. Oxide-Driven Carbon Nanotube Growth in Supported Catalyst CVD. *J. Am. Chem. Soc.* **2007**, *129*, 15772–15773.
17. Song, J.; Du, G.; Song, C.; Zhao, J.; Feng, S.; Zheng, J.; Zhu, Z. Identification and Technical Accessibility of the Carbon Self-Assembly Concept Hidden in Catalytic Carbon Nanotube Evolution. *J. Mater. Chem.* **2009**, *41*, 7725–7729.
18. Schäffel, F.; Kramberger, C.; Rümmeli, M. H.; Grimm, D.; Mohn, E.; Gemming, T.; Pichler, T.; Rellinghaus, B.; Büchner, B.; Schultz, L. Nanoengineered Catalyst Particles as a Key for Tailor-Made Carbon Nanotubes. *Chem. Mater.* **2007**, *19*, 5006–5009.
19. Rümmeli, M. H.; Kramberger, C.; Löffler, M.; Jost, O.; Bystrzejewski, M.; Grueneis, A.; Gemming, T.; Pompe, W.; Büchner, B.; Pichler, T. Catalyst Volume to Surface Area Constraints for Nucleating Carbon Nanotubes. *J. Phys. Chem. B* **2007**, *111*, 8234–8241.
20. Dai, H.; Rinzler, A.; Nikolaev, P.; Thess, A.; Colbert, D.; Smalley, R. E. Single-Wall Nanotubes Produced by Metal-Catalyzed Disproportionation of Carbon Monoxide. *Chem. Phys. Lett.* **1996**, *260*, 471–475.
21. Rodríguez-Manzo, J. A.; Terrones, M.; Terrones, H.; Kroto, H. W.; Sun, L.; Banhart, F. *In Situ* Nucleation of Carbon Nanotubes by the Injection of Carbon Atoms into Metal Particles. *Nat. Nanotechnol.* **2007**, *2*, 307–311.

22. Yoshida, H.; Takeda, S.; Uchiyama, T.; Kohno, H.; Homma, Y. Atomic-Scale *In-Situ* Observation of Carbon Nanotube Growth from Solid State Iron Carbide Nanoparticles. *Nano Lett.* **2008**, *8*, 2082–2086.
23. Hofmann, S.; Blume, R.; Wirth, C.; Cantoro, M.; Sharma, R.; Ducati, C.; Hävecker, M.; Zafeiratos, S.; Schnörch, P.; Östereich, A.; *et al.* State of Transition Metal Catalysts during Carbon Nanotube Growth. *J. Phys. Chem. C* **2009**, *113*, 1648–1656.
24. Hofmann, S.; Sharma, R.; Ducati, C.; Du, G.; Mattevi, C.; Cepek, C.; Cantoro, M.; Pisana, S.; Parvez, A.; Cervantes-Sodi, F.; *et al. In Situ* Observations of Catalyst Dynamics during Surface-Bound Carbon Nanotube Nucleation. *Nano Lett.* **2007**, *7*, 602–608.
25. José-Yacamán, M.; Miki-Yoshida, M.; Rendón, L. Catalytic Growth of Carbon Microtubules with Fullerene Structure. *Appl. Phys. Lett.* **1993**, *62*, 657–659.
26. Jackson, D. S.; Hargreaves, S. J. S. *Metal Oxide Catalysis*; Wiley-VCH: Weinheim, Germany, 2009.
27. Somorjai, G. A. Molecular Chemistry and Catalysis by Surfaces. *Chem. Eng. News* **2008**, *86*, 15–21.
28. Rümmeli, M. H.; Kramberger, C.; Grüneis, A.; Ayala, A.; Gemming, T.; Büchner, B.; Pichler, T. On the Graphitization Nature of Oxides for the Formation of Carbon Nanostructures. *Chem. Mater.* **2007**, *19*, 4105–4107.
29. Kusunoki, M.; Suzuki, T.; Hirayama, T.; Shibata, N.; Kaneko, K. A Formation Mechanism of Carbon Nanotube Films on SiC(0001). *Appl. Phys. Lett.* **2000**, *77*, 531–533.
30. Lu, W.; Boeckl, J.; Mitchel, W. C.; Rigueur, J.; Collins, W. E. Role of Oxygen in Growth of Carbon Nanotubes on SiC. *Mater. Sci. Forum* **2006**, *527*, 1575–1578.
31. Hata, K.; Futaba, D. N.; Mizuno, K.; Namai, T.; Yumura, M.; Iijima, S. Water-Assisted Highly Efficient Synthesis of Impurity-Free Single-Walled Carbon Nanotubes. *Science* **2004**, *306*, 1362–1364.
32. Yamada, T.; Maigne, A.; Yudasaka, M.; Mizuno, K.; Futaba, D.; Yumura, M.; Iijima, S.; Hata, K. Revealing the Secret of Water-Assisted Carbon Nanotube Synthesis by Microscopic Observation of the Interaction of Water on the Catalysts. *Nano Lett.* **2008**, *8*, 4288–4292.
33. Fu, Q.; Wagner, T. Interaction of Nanostructured Metal Overlayers with Oxide Surfaces. *Surf. Sci. Rep.* **2007**, *62*, 431–498.